Equivalence of digital image correlation criteria for pattern matching

Bing Pan,[1,*] Huimin Xie,[2] and Zhaoyang Wang[3]

[1]Institute of Solid Mechanics, Beijing University of Aeronautics & Astronautics, Beijing 100191, China

[2]School of Aerospace, Tsinghua University, Beijing 100083, China

[3]Department of Mechanical Engineering, The Catholic University of America, Washington, DC 20064, USA

*Corresponding author: panb04@mails.tsinghua.edu.cn

Received 21 May 2010; revised 18 August 2010; accepted 24 August 2010;
posted 7 September 2010 (Doc. ID 128721); published 30 September 2010

In digital image correlation (DIC), to obtain the displacements of each point of interest, a correlation criterion must be predefined to evaluate the similarity between the reference subset and the target subset. The correlation criterion is of fundamental importance in DIC, and various correlation criteria have been designed and used in literature. However, little research has been carried out to investigate their relations. In this paper, we first provide a comprehensive overview of various correlation criteria used in DIC. Then we focus on three robust and most widely used correlation criteria, i.e., a zero-mean normalized cross-correlation (ZNCC) criterion, a zero-mean normalized sum of squared difference (ZNSSD) criterion, and a parametric sum of squared difference ($PSSD_{ab}$) criterion with two additional unknown parameters, since they are insensitive to the scale and offset changes of the target subset intensity and have been highly recommended for practical use in literature. The three correlation criteria are analyzed to establish their transversal relationships, and the theoretical analyses clearly indicate that the three correlation criteria are actually equivalent, which elegantly unifies these correlation criteria for pattern matching. Finally, the equivalence of these correlation criteria is further validated by numerical simulation and actual experiment.

OCIS codes: 100.4999, 120.6650.

1. Introduction

Digital image correlation (DIC) [1–6] is a noncontact, full-field optical metrology for accurate measurements of two-dimensional (2D) and three-dimensional (3D) deformation and shape from digital images of test object surface recorded at different configurations. In recent years, DIC has acquired more and more attention and been increasingly used in various scientific fields and engineering applications, due to its advantages of simple experimental setup and specimen preparation, low requirements on measurement environment, and wide range of measurement sensitivity and resolution [6].

In essence, DIC is an optical method based on digital image processing and numerical computing. It takes advantage of the artificial speckle pattern or natural surface texture on the test object surface as a carrier of deformation information, and it tracks the motion of each concerned pixel of the reference image in the deformed image. To this end, a reference subset containing sufficient local intensity variations centered at the interrogated pixel is selected first. Then, by means of a predefined criterion and a certain optimization algorithm [4–8], the DIC technique searches the deformed image for the target (or deformed) subset, whose intensity pattern is of maximum similarity (or minimum difference) with the reference subset. The predefined criterion can be a cross-correlation criterion or a sum of squared difference criterion [6]. Since the matching process of DIC cannot be fulfilled without a predefined criterion, the

0003-6935/10/285501-09$15.00/0

correlation criterion (or matching criterion) is of fundamental importance in DIC. As pointed out in a recent book, "the digital image correlation method owes its name to the use of the normalized cross-correlation criterion" [5], thus it can be seen that the significance of correlation criterion in DIC technique is self-evident.

In literature, various criteria, including cross-correlation (CC) criterion, sum of absolute difference (SAD), sum of squared difference (SSD), and parametric sum of squared difference (PSSD) have been designed and used [4,6,9–17]. It should be emphasized here, first, that the selection of correlation criterion for matching is not an important issue if the intensity of each pixel does not change in the deformed image (though the position of the same pixel changes due to external loading). Recently, an evaluation of four SSD criteria for displacement and strain mapping was carried out by W. Tong [11], and the result shows that various correlation criteria almost yield the same results under the condition that the intensity value of each pixel remains unchanged in the deformed image. However, this ideal condition hardly holds true in practical experiments, where the intensity of the deformed image may undergo potential undesired changes. In certain cases, the local intensity within the target image may differ significantly with that of the reference image, and the intensity changes between images may be induced by various reasons. For example, the illumination lighting may be uneven and fluctuate with time. The reflectivity of the test specimen surface may also change due to an increase of surface roughness accompanying the increasing strain. In particular, in 3D DIC based on the stereovision principle, the same specimen surface image captured by different cameras may differ with each other due to different imaging orientations [5]. Additionally, in the correlation of projected speckle patterns, the different reflectance of the reference plane and the test object's surface may also lead to notable variations in the recorded images [18]. In all the above situations, a robust correlation criterion must be used to accommodate the variations in the intensity of the deformed image, otherwise significant displacement measurement errors may occur due to the mismatch of intensity change model [11,16,17].

Based on the consideration of compensating for or eliminating the errors associated with intensity change of the target subset, a zero-mean cross-correlation criterion (ZNCC), a zero-mean normalized sum of squared difference (ZNSSD) criterion, and a parametric sum of squared difference ($PSSD_{ab}$) criterion with two additional unknown parameters (compared with a conventional SSD criterion) have been highly recommended for matching the same subsets located in the reference image and the deformed image, as they are insensitive to the potential scale and offset changes of the target subset intensity. The mathematical expressions of the above-mentioned three correlation criteria are fully different, though these three correlation criteria have the same performance against the offset and scale changes in the deformed subset intensity. Accordingly, understanding the transversal relationships among them is undoubtedly an interesting and meaningful issue and also useful to the optimal use of these matching criteria.

In this work, we first provide a comprehensive overview of the various correlation criteria used in DIC for quantitatively evaluating the similarity or difference between the reference subset and the target subset. Then, we focus on the three robust and most widely used correlation criteria, i.e., the ZNCC criterion, the ZNSSD criterion, and the $PSSD_{ab}$ criterion. The three correlation criteria are analyzed to establish their transversal relationships, and the analysis clearly indicates that the three correlation criteria are indeed equivalent, which elegantly unifies these popular correlation criteria for pattern matching. Finally, both numerical and actual experiments were carried out to validate the correctness of the theoretical derivations, and the results show good agreement with theoretical predictions.

2. Basic Principle of Digital Image Correlation

The basic principle of DIC is the tracking (or matching) of the same image points located in the two digital images of the test specimen surface recorded before and after deformation [6]. It should be noted first that the test specimen surface must be covered with a random speckle pattern in the DIC technique, which serves as a carrier of deformation information [19–21]. As can be seen from Fig. 1, in order to compute the displacements of a point of interest $P(x_0, y_0)$, a square reference subset of $N \times N$ pixels centered at the interrogated point P from the reference image is chosen and used to track its corresponding location in the deformed image. To accurately track the

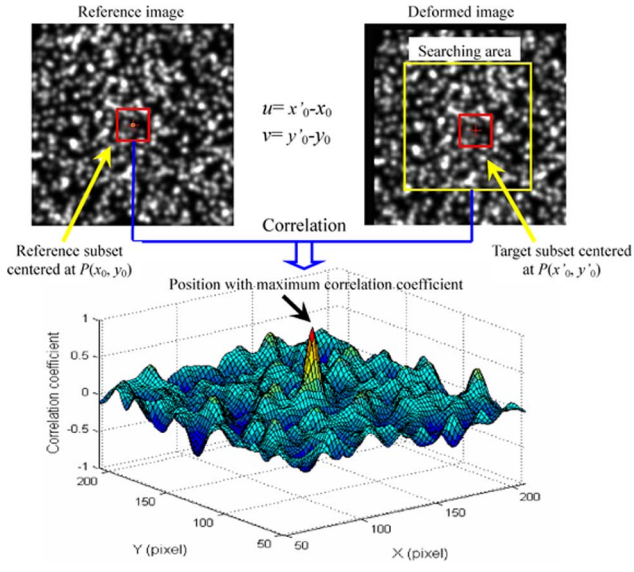

Fig. 1. (Color online) Example of tracking the reference subset in the deformed image using DIC. The center position of the target subset is obtained through searching the peak position of the distribution of the correlation coefficient.

position of the reference subset in the deformed image, a criterion must be established to evaluate the similarity or difference between the selected reference subset and the target subset. By sliding the reference subset in the searching area of the deformed image and computing the correlation coefficient at each location, a correlation coefficient map is obtained as schematically illustrated in Fig. 1. Subsequently, the matching procedure is completed through searching for the peak position of the distribution of correlation coefficient using certain optimization algorithm. Once the correlation coefficient extreme is detected, the position of the deformed subset can be determined. The differences of the positions of the reference subset center and the target subset center yield the in-plane displacement vector at the point P. The same procedure is repeated for other pixels of interest to obtain the full-field displacement.

3. Overview of Various Correlation Criteria for Digital Image Correlation

To evaluate the similarity (or difference) degree between the reference subset and its deformed counterpart, correlation criteria must be defined in advance, which plays a critical role in DIC. Generally speaking, the various correlation criteria can be classified into the following four categories, according to their mathematical definitions, i.e., cross-correlation (CC), sum of absolute difference (SAD), sum of squared difference (SSD), and parametric sum of squared difference (PSSD) [14–17]. In this paper, we will focus on CC, SSD, and PSSD criteria and neglect SAD criteria, as SAD criteria are less practical and seldom used in comparison with the other three types of correlation criteria. As we know, the correlation coefficient is computed between the reference subset and target subset. For a square subset containing $n(=N\times N)$ discrete pixels, let $f(x_i,y_i)$ and $g(x_i',y_i')$ denote the gray values of the ith pixel of the reference subset and the target subset, respectively. For the purpose of notation brevity and clarity, the gray values of $f(x_i,y_i)$ and $g(x_i',y_i')$ are further simplified as f_i and g_i. The lower and upper bounds of summation are also omitted in all the following derivations for the same purpose.

A. Cross-Correlation Criteria

Basically, the commonly used CC criteria can be further categorized into four types, according to their performance against the possible intensity changes presented in the target subset. All the CC criteria involve maximizing the corresponding cross-correlation coefficients.

The direct CC coefficient is defined as

$$C_{\mathrm{CC}}=\sum f_i g_i. \tag{1}$$

It is necessary to note that the computation of a CC coefficient can be performed either in the spatial domain or in the Fourier space by using FFT [22–24].

By subtracting the mean value of the subset intensity, the zero-mean cross-correlation (ZCC) coefficient is of the following form:

$$C_{\mathrm{ZCC}}=\sum[(f_i-\bar{f})(g_i-\bar{g})], \tag{2}$$

where $\bar{f}=\frac{1}{n}\sum_{i=1}^{n}f_i$ and $\bar{g}=\frac{1}{n}\sum_{i=1}^{n}g_i$ denote the ensemble averages of the reference and target subsets, respectively. Since the mean value of the subset intensity has been removed, the ZCC criterion is tolerant of the offset change of the deformed image.

Similarly, by dividing the root-sum-square of the subset intensity, the normalized cross-correlation (NCC) coefficient is defined as

$$C_{\mathrm{NCC}}=\frac{\sum f_i g_i}{\sqrt{\sum f_i^2\sum g_i^2}}. \tag{3}$$

It is worth mentioning that $1-C_{\mathrm{NCC}}$ has also been used in literature instead of C_{NCC} [4,7].

Finally, combining the advantages of ZCC and NCC criteria, the zero-mean normalized cross-correlation (ZNCC) coefficient can be given as

$$C_{\mathrm{ZNCC}}=\frac{\sum \bar{f}_i\bar{g}_i}{\sqrt{\sum \bar{f}_i^2\sum \bar{g}_i^2}}, \tag{4}$$

where $\bar{f}_i=f_i-\bar{f}$ and $\bar{g}_i=g_i-\bar{g}$. It is clear that the computation complexity of Eq. (4) is greater than other CC criteria. Recently, research has also been conducted to speed the calculation of the ZNCC criterion [25–27].

The ZNCC criterion is highly recommended for practical use, as it is insensitive to the offset and scale changes in the intensity of the target subset and provides the most accurate and reliable displacement estimations compared with other CC criteria [11,28]. In other words, if a linear transformation of the target subset gray intensity has been made according to function $g_i'=a\times g_i+b$, the resulting ZNCC coefficient remains unchanged.

B. Sum of Squared Difference Criteria

Mathematically, maximization of the above CC criteria is actually equivalent to the minimization of the corresponding SSD criterion. That is to say, subset matching can be intuitively achieved by minimizing the difference between the reference and target subsets. For instance, the direct SSD criterion (which corresponds to the direct CC criterion) involves minimizing the following formulation:

$$C_{\mathrm{SSD}}=\sum(f_i-g_i)^2. \tag{5}$$

It is noteworthy that a slightly different SSD criterion, in the form of $\sum(f_i-g_i)^2/\sum f_i^2$, has been used in Refs. [4,11,29–32]. However, because the

denominator $\sum f_i^2$ is a constant for each reference subset, it can be directly neglected without any consequence. Therefore, we do not consider that correlation criterion as a new one in this work.

The zero-mean sum of squared difference (ZSSD) criterion (which corresponds to the ZCC criterion), which is insensitive to the offset change of the intensity of the target subset, is to minimize the following coefficient:

$$C_{\mathrm{ZSSD}} = \sum[(f_i - \bar{f}) - (g_i - \bar{g})]^2. \tag{6}$$

The coefficient of the normalized sum of squared difference (NSSD) criterion (which corresponds to the NCC criterion), which is insensitive to scale change of the intensity of the target subset, can be expressed as

$$C_{\mathrm{NSSD}} = \sum\left(\frac{f_i}{\sqrt{\sum f_i^2}} - \frac{g_i}{\sqrt{\sum g_i^2}}\right)^2. \tag{7}$$

Last, the coefficient of the ZNSSD criterion (which corresponds to the ZNCC criterion), which is insensitive to both offset and scale changes of the intensity of the target subset [11,28], is defined as

$$C_{\mathrm{ZNSSD}} = \sum\left(\frac{\bar{f}_i}{\sqrt{\sum \bar{f}_i^2}} - \frac{\bar{g}_i}{\sqrt{\sum \bar{g}_i^2}}\right)^2. \tag{8}$$

C. Parametric Sum of Squared Difference Criteria

As described previously, the direct SSD criterion is a very simple and intuitive approach for subset matching, but its limitation is the incapability of coping with the change of the intensity of the target subset. To solve this problem and accommodate the intensity change of the target subset, a few different kinds of SSD criteria that incorporate additional parameters into the coefficient definition have been developed [5,14–17]. These criteria are referred to as parametric sum of squared difference (PSSD) criteria in this work.

When an unknown parameter b is incorporated into the SSD coefficient to account for the offset change of the intensity of the target subset [5,14–17], the new criterion is named the PSSD_b criterion hereafter. The PSSD_b coefficient is expressed as

$$C_{\mathrm{PSSD}b} = \sum(f_i + b - g_i)^2. \tag{9}$$

It is worth noting that the above coefficient has been used by Vendroux and Knauss [31], in the form of $\sum(f_i + b - g_i)^2 / \sum f_i^2$, to measure the submicrometer deformation by combining DIC and a scanning tunneling microscope (STM) where b denotes a global offset in height between the two scans of the STM.

In a similar manner, the PSSD_a criterion incorporates an unknown parameter a to account for the scale change of the intensity of target subset [5,16,17], and the coefficient is defined as

$$C_{\mathrm{PSSD}a} = \sum(af_i - g_i)^2. \tag{10}$$

The generalized PSSD_{ab} coefficient considers two unknown parameters a and b to account for both the offset and scale changes of the intensity of the target subset [5,14–17], and it is given as

$$C_{\mathrm{PSSD}ab} = \sum(af_i + b - g_i)^2. \tag{11}$$

All of the above PSSD coefficients can be normalized to a certain extent by dividing $\sum f_i^2$. However, as mentioned previously, this manipulation does not improve the convergence characteristics of the criteria, since the denominator $\sum f_i^2$ for a subset remains constant.

4. Equivalence of Correlation Criteria Used for Pattern Matching

In the text below, the relationships among the ZNCC, ZNSSD, and PSSD_{ab} criteria are described. It should be noted that the derivations can also be easily applied to other simpler correlation criteria, and similar relationships can be established.

A. From ZNSSD Criterion to ZNCC Criterion

It is easy to show that the ZNSSD coefficient is directly related to the ZNCC coefficient [11,28] as follows:

$$\begin{aligned} C_{\mathrm{ZNSSD}} &= \sum\left(\frac{\bar{f}_i}{\sqrt{\sum \bar{f}_i^2}} - \frac{\bar{g}_i}{\sqrt{\sum \bar{g}_i^2}}\right)^2 \\ &= \sum\left(\frac{\bar{f}_i^2}{\sum \bar{f}_i^2} - 2\frac{\bar{f}_i \bar{g}_i}{\sqrt{\sum \bar{f}_i^2}\sqrt{\sum \bar{g}_i^2}} + \frac{\bar{g}_i^2}{\sum \bar{g}_i^2}\right) \\ &= 2 - 2\frac{\sum \bar{f}_i \bar{g}_i}{\sqrt{\sum \bar{f}_i^2}\sqrt{\sum \bar{g}_i^2}} = 2(1 - C_{\mathrm{ZNCC}}). \end{aligned} \tag{12}$$

In practice, because the optimization of the ZNSSD coefficient is relatively easier than that of the ZNCC coefficient, the ZNSSD criterion is usually employed. However, in certain DIC approaches, such as the recently developed reliability-guided digital image correlation (RG-DIC) method [33–35], the ZNCC coefficient is preferred for intuitively showing the effect and reliability of subset matching because it falls into a range of $[-1, 1]$, whereas the ZNSSD coefficient has a range of $[0, 4]$. In this case, the ZNSSD criterion can be employed for subset correlation optimization, after which the corresponding ZNCC coefficient can be calculated according to the following equation of $C_{\mathrm{ZNCC}} = 1 - \frac{C_{\mathrm{ZNSSD}}}{2}$ to guide the DIC calculation path.

B. From PSSD_{ab} Criterion to ZNCC Criterion

Although the PSSD_{ab} coefficient defined by Eq. (11) has a substantially different form from the ZNCC coefficient defined by Eq. (4), we will show below that

the PSSD_{ab} criterion is equivalent to the ZNCC criterion.

By minimizing the PSSD_{ab} coefficient with respect to a and b, we have

$$\begin{cases} \frac{\partial C_{\mathrm{PSSD}ab}}{\partial a} = 0 \\ \frac{\partial C_{\mathrm{PSSD}ab}}{\partial b} = 0 \end{cases} \Rightarrow \begin{cases} 2\sum[(af_i + b - g_i)f_i] = 0 \\ 2\sum(af_i + b - g_i) = 0 \end{cases}. \quad (13)$$

Solving Eq. (13), the optimal estimates for a and b are determined as

$$a = \frac{\sum[(g_i - b)f_i]}{\sum f_i^2}, \quad (14)$$

$$b = \frac{\sum(g_i - af_i)}{\sum 1} = \frac{\sum(g_i - af_i)}{n} = \bar{g} - a\bar{f}. \quad (15)$$

Substituting Eq. (15) into Eq. (14), the unknown parameter a can be determined as

$$\begin{aligned} a &= \frac{\sum[(g_i - \bar{g} + a\bar{f})f_i]}{\sum f_i^2} \Rightarrow a\sum f_i^2 \\ &= \sum[(g_i - \bar{g} + a\bar{f})f_i] \Rightarrow a = \frac{\sum[(g_i - \bar{g})f_i]}{\sum[(f_i - \bar{f})f_i]} = \frac{\sum \bar{g}_i f_i}{\sum \bar{f}_i f_i}. \end{aligned} \quad (16)$$

It is easy to prove that $\sum \bar{g}_i f_i = \sum \bar{g}_i \bar{f}_i$ and $\sum \bar{f}_i f_i = \sum \bar{f}_i^2$, thus a and b can be further expressed as

$$a = \frac{\sum \bar{g}_i \bar{f}_i}{\sum \bar{f}_i^2}, \quad (17)$$

$$b = \bar{g} - \frac{\sum \bar{g}_i \bar{f}_i}{\sum \bar{f}_i^2}\bar{f}. \quad (18)$$

By substituting Eqs. (15) and (17) into Eq. (11), the PSSD_{ab} coefficient now can be further denoted as

$$\begin{aligned} C_{\mathrm{PSSD}ab} &= \sum(af_i + b - g_i)^2 = \sum(af_i + \bar{g} - a\bar{f} - g_i)^2 \\ &= \sum(a\bar{f}_i - \bar{g}_i)^2 = \sum\left(\frac{\sum \bar{g}_i \bar{f}_i}{\sum \bar{f}_i^2}\bar{f}_i - \bar{g}_i\right)^2 \\ &= \sum\left[\left(\frac{\sum \bar{g}_i \bar{f}_i}{\sum \bar{f}_i^2}\right)^2 \bar{f}_i^2 - 2\frac{\sum \bar{g}_i \bar{f}_i}{\sum \bar{f}_i^2}\bar{f}_i \bar{g}_i + \bar{g}_i^2\right] \\ &= -\frac{(\sum \bar{g}_i \bar{f}_i)^2}{\sum \bar{f}_i^2} + \sum \bar{g}_i^2 \\ &= \sum \bar{g}_i^2\left[1 - \frac{(\sum \bar{g}_i \bar{f}_i)^2}{\sum \bar{g}_i^2 \sum \bar{f}_i^2}\right] = \sum \bar{g}_i^2(1 - C_{\mathrm{ZNCC}}^2). \end{aligned} \quad (19)$$

Although the PSSD_{ab} criterion does not have a linear relationship with the ZNCC criterion as explicitly shown in Eq. (19), mathematic deduction will show that their partial derivatives with respect to the desired deformation parameter vector has a simple linear relationship, considering if we take $\sum \bar{g}_i^2$ as constant. Besides, upon a successfully subset matching using either the PSSD_{ab} or the ZNCC criteria, the value of $\sum \bar{g}_i^2$ can be readily determined by virtue ofa certain interpolation scheme (e.g., a bicubic interpolation [36]). Consequently, the PSSD_{ab} and ZNCC coefficients can be obtained from each other with Eq. (19) or the following formula:

$$C_{\mathrm{ZNCC}} = \sqrt{1 - \frac{C_{\mathrm{PSSD}ab}}{\sum \bar{g}_i^2}}. \quad (20)$$

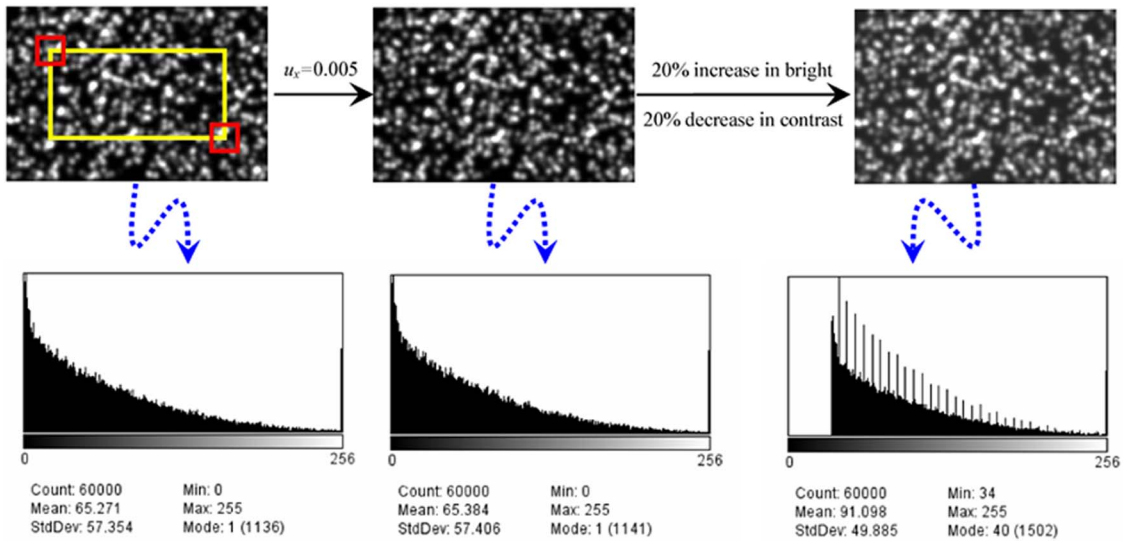

Fig. 2. (Color online) Reference image (left), deformed image (middle), and deformed image after artificially adjusted with 20% increase in brightness and 20% decreases in contrast (right) and their histograms. The rectangle of the reference image indicates the specified region of interest, and the two small squares denote the subset used for calculation.

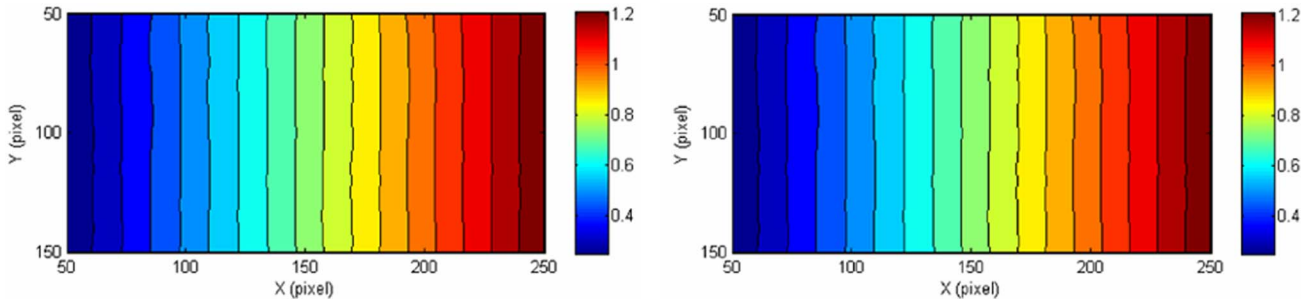

Fig. 3. (Color online) Computed u-field displacements by using the ZNSSD criterion (a) and the PSSD_{ab} criterion (b) for a simulated uniaxial tensile test.

In the RG-DIC technique, the ZNCC coefficient is typically employed to guide the DIC calculation path. With the PSSD_{ab} criterion, we can also convert the PSSD_{ab} coefficient to the ZNCC coefficient easily using Eq. (20) after each optimization to determine the calculation path using ZNCC coefficients.

5. Verification by Numerical Simulation

A. Computer-Simulated Speckle Images

In this section, computer-simulated speckle patterns with controllable deformation are used to verify the presented mathematical derivations. First, a reference image with a resolution of 300×200 pixels and a pixel depth of 8 bit gray scale is generated using the simulation algorithm in Ref. [8]. The detailed parameters used in simulation are the speckle granule radius $R = 4$ pixels and the total number of speckle granules $s = 1000$. Then, the reference speckle pattern is numerically stretched in the x direction with parameter $u_x = 0.005$ and other displacement parameters being 0 to get the deformed image. Furthermore, to simulate less ideal experimental conditions with illumination intensity variations, the intensity of the deformed image is artificially adjusted with a 20% increase in brightness and a 20% decrease in contrast. Figure 2 shows the reference speckle image, the deformed speckle image, and the final speckle image with artificially changed intensity. The corresponding histograms are also shown in the figure, from which the induced intensity variations can be clearly seen.

To verify the equivalence and investigate the computational efficiency of the three robust DIC criteria, the x directional displacement field of the aforementioned deformed image (i.e., the right-side images of Fig. 2) is computed through optimizing the ZNSSD criterion and PSSD_{ab} criterion, respectively, using the Newton–Raphson algorithm with the first-order shape function. During optimization, bicubic interpolation is adopted to reconstruct the intensity and intensity gradients at subpixel locations. Here, it should be noted that the DIC technique employing certain interpolation schemes, including the bicubic interpolation, will usually give rise to periodic bias error in the determined displacements [37,38]. Detailed implementation algorithms for the ZNSSD criterion and PSSD_{ab} criterion can be found in our previous works [28,17]. Since the ZNCC criterion has a simple linear relationship with the ZNSSD criterion, implementation of the ZNCC criterion will not be provided below. In the following analysis, the displacements are calculated with a subset of 31×31 pixels and a grid step (the distance between two adjacent pixels being computed) of five pixels between consecutive calculation points.

B. Equivalence of ZNSSD and PSSD_{ab} Criteria

The resulting u-field displacements and ZNCC coefficient distributions, converted from the ZNSSD

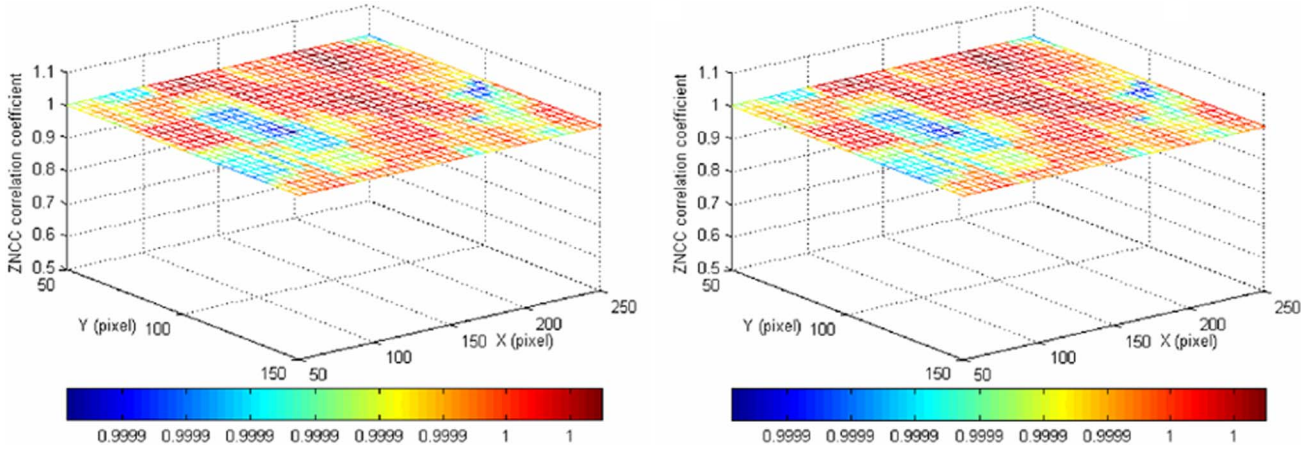

Fig. 4. (Color online) Computed ZNCC coefficients by using the ZNSSD criterion (a) and the PSSD_{ab} criterion (b) for a simulated uniaxial tensile test.

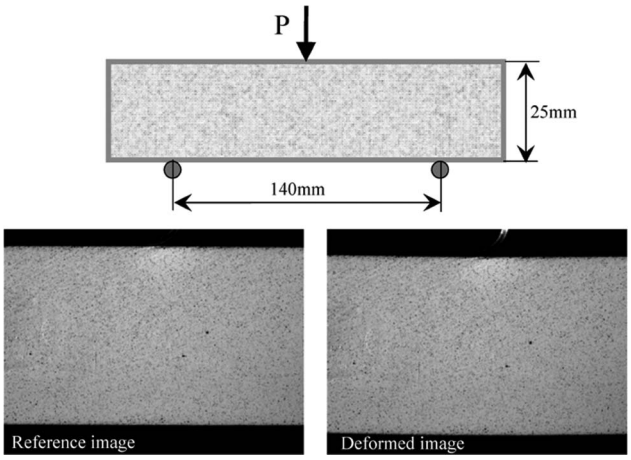

Fig. 5. Schematic of a three-point bending experiment (top) and the captured reference and deformed images (bottom).

coefficient according to Eq. (12) and the PSSD_{ab} coefficient according to Eq. (20), are shown in Figs. 3 and 4, respectively. Although the intensity distribution of the deformed image is substantially changed from the reference image, the measured displacements are in good agreement with the imposed theoretical values, which clearly demonstrate the robustness of the ZNSSD and PSSD_{ab} criteria. Meanwhile, the displacement results and the ZNCC coefficients obtained from two criteria are identical, and no differences can be observed. The experimental results clearly verify the correctness of the above derivations and the equivalence of the three correlation criteria.

C. Computational Efficiency of ZNSSD and PSSD_{ab} Criteria

As can be seen from Eq. (8), the mean value (i.e., $\bar{f}_i$ and $\bar{g}_i$) and root-sum-square of subset intensity variations (i.e., $\sqrt{\sum \tilde{f}_i^2}$ and $\sqrt{\sum \tilde{g}_i^2}$) must be provided during the optimization of the ZNSSD criterion. As a consequence, the optimization of PSSD_{ab} is much easier than that of the ZNSSD criterion, despite that the PSSD_{ab} criterion involves two more unknown parameters (i.e., a and b). Let us take the simulated experiment in Section 5.B as an example. Totally, $861 (= 21 \times 41)$ points in the reference image were calculated using a DIC program written in C++ and a Dell Vostro 1520 laptop computer (2.40 GHz Intel Core 2 Duo processor and 4 GB memory). The whole computation times for the ZNSSD criterion and PSSD_{ab} criterion are 3.2 and 1.5 s, respectively. The results show that the computational efficiency of PSSD_{ab} is higher than that of the ZNSSD criterion. However, it is important to point out that the computation time shows only the relative performance of one algorithm versus the other and is not an absolute time, which depends on a number of factors, such as programming efficiency, hardware performance, use of program language and subpixel interpolation scheme, and the problem itself.

6. Verification by Actual Experiment

A three-point bending test was also performed to verify the correctness of the mathematical derivation. The specimen was made of polymethyl methacrylate (PMMA) material with Young's modulus $E = 4.0$ Gpa and Poisson's ratio $v = 0.35$. Its geometry and loading condition are schematically shown in Fig. 5. Figure 5 also illustrates the reference image recorded before loading and a deformed image acquired after exerting a 700 N load. The recorded digital images are of 768×576 pixels in resolution and 256 gray levels in color depth.

A rectangular area in the middle of the reference image is chosen to be the region of interest. The displacements were calculated at a mesh of 36×60 points (which corresponds to an area of 350 pixels $\times$ 590 pixels) with a subset size of 39×39 pixels and a grid step of 10 pixels. Totally, the displacement components of 2160 discrete points were analyzed and computed through optimizing the ZNSSD criterion and PSSD_{ab} criterion, respectively, using the same DIC code. The computed u-displacement field, v-displacement field, and ZNCC coefficient distribution by optimizing the ZNSSD criterion and PSSD_{ab} criterion are shown in Figs. 6 and 7, respectively. It is seen that there are no discernable differences between the two results. A quantitative comparison between two computations shows that the absolute

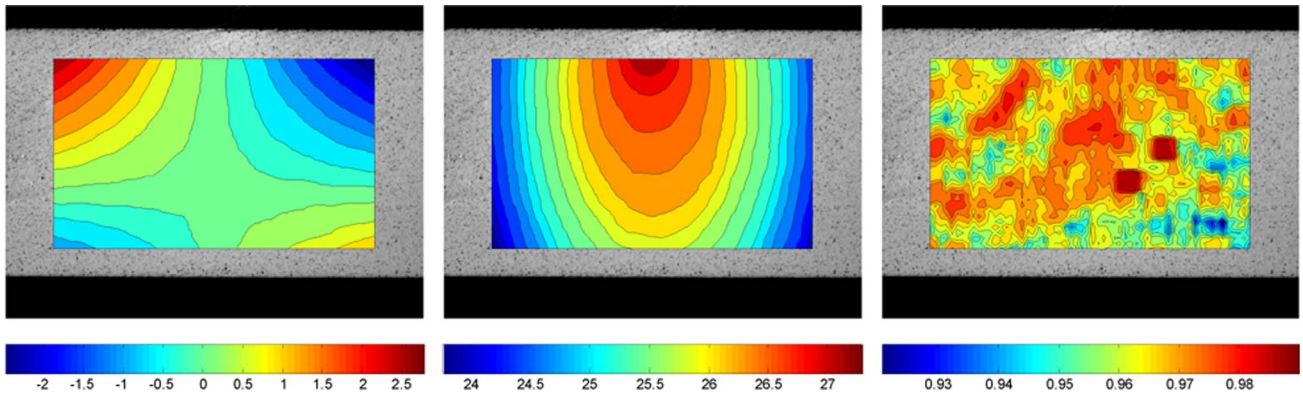

Fig. 6. (Color online) Computed u-displacement (left), v-displacement (middle), and ZNCC coefficient distribution (right) by optimizing the ZNSSD criterion for a three-point bending test.

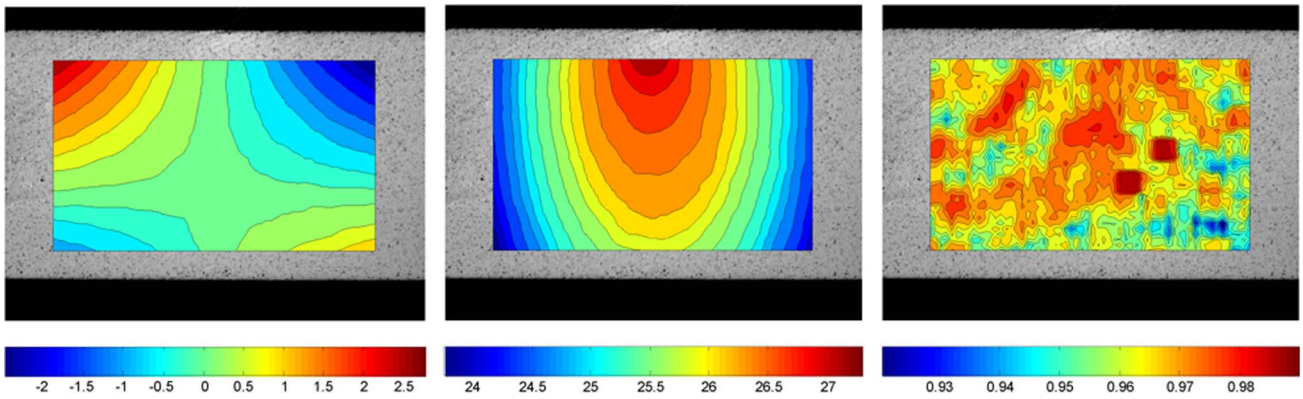

Fig. 7. (Color online) Computed u-displacement (left), v-displacement (middle), and the ZNCC coefficient distribution (right) by optimizing the PSSD_{ab} criterion for a three-point bending test.

maximum differences in the u-displacement, v-displacement, and ZNCC correlation coefficient are 0.016, 0.015, and 0.0005 pixels, respectively. The minor differences may be caused by the different calculation scheme used and are acceptable in most calculations. As for the computation efficiency, we draw a similar conclusion under the same computation conditions. The computation times for the ZNSSD criterion and PSSD_{ab} criterion are 14.9 and 9.3 s, respectively.

7. Conclusion

Various correlation criteria used in DIC for evaluating the intensity pattern similarity (or difference) between the reference subset and the target subset are reviewed, and these criteria are classified into four types to provide the users of DIC a clear image of their mathematical definitions and mutual relationships. Among these correlation criteria, the ZNCC criterion, the ZNSSD criterion, and the PSSD_{ab} criterion with two additional unknown parameters have been strongly recommended for practical use, since they are insensitive to the scale and offset changes of the deformed image. In this work, their transversal relationships are established through rigorous mathematical derivation and verified by computer simulation and actual experiment. It is indicated that the three correlation criteria are actually equivalent and are thus elegantly unified for pattern matching. However, a comparison of computational times in this work shows that the PSSD_{ab} criterion with two additional unknown parameters is a little faster than the other correlation criteria.

This work is supported by the National Natural Science Foundation of China (NSFC) under grant 11002012, and the Science Fund of State Key Laboratory of Automotive Safety and Energy under grant KF10041.

References

1. W. H. Peters and W. F. Ranson, "Digital imaging techniques in experimental stress analysis," Opt. Eng. **21**, 427–431 (1982).
2. T. C. Chu, W. F. Ranson, M. A. Sutton, and W. H. Peters, "Applications of digital-image-correlation techniques to experimental mechanics," Exp. Mech. **25**, 232–244 (1985).
3. R. S. Sirohi, *Optical Methods of Measurement: Wholefield Techniques*, 2nd ed. (CRC, 2009).
4. M. A. Sutton, S. R. McNeill, J. D. Helm, and Y. J. Chao, *Advances in Two-Dimensional and Three-Dimensional Computer Vision*, P. K. Rastogi, ed., Topics in Applied Physics (Springer–Verlag, 2000), Vol. 77, pp. 323–372.
5. M. A. Sutton, J. J. Orteu, and H. W. Schreier, *Image Correlation for Shape, Motion, and Deformation Measurements* (Springer, 2009).
6. B. Pan, K. M. Qian, H. M. Xie, and A. Asundi, "Two-dimensional digital image correlation for in-plane displacement and strain measurement: a review," Meas. Sci. Technol. **20**, 062001 (2009).
7. H. A. Bruck, S. R. McNeil, M. A. Sutton, and W. H. Peters, "Digital image correlation using Newton–Raphson method of partial differential correction," Exp. Mech. **29**, 261–267 (1989).
8. B. Pan, H. M. Xie, B. Q. Xu, and F. L. Dai, "Performance of subpixel registration algorithms in digital image correlation," Meas. Sci. Technol. **17**, 1615–1621 (2006).
9. A. Giachetti, "Matching techniques to compute image motion," Image Vis. Comput. **18**, 247–260 (2000).
10. S. P. Ma and G. C. Jin, "New correlation coefficients designed for digital speckle correlation method (DSCM)," Proc. SPIE **5058**, 25–33 (2003).
11. W. Tong, "An evaluation of digital image correlation criteria for strain mapping applications," Strain **41**, 167–175 (2005).
12. P. Zhou and K. E. Goodson, "Subpixel displacement and deformation gradient measurement using digital image/speckle correlation," Opt. Eng. **40**, 1613–1620 (2001).
13. M. Z. Brown, D. Burschka, and G. D. Hager, "Advances in computational stereo," IEEE Trans. Pattern Anal. Mach. Intell. **25**, 993–1008 (2003).
14. A. W. Gruen, "Adaptive least squares correlation: a powerful image matching technique," S. Afr. J. Photogr. Rem. Sensing Cartogr. **14**(3), 175–187 (1985).
15. Y. Altunbasak, R. M. Mersereau, and A. J. Patti, "A fast parametric motion estimation algorithm with illumination and lens distortion correction," IEEE Trans. Image Process. **12**, 395–408 (2003).
16. B. Pan, A. Asundi, H. M. Xie, and J. X. Gao, "Digital Image correlation using iterative least squares and pointwise least squares for displacement field and strain field measurements," Opt. Lasers Eng. **47**, 865–874 (2009).
17. B. Pan, Z. Y. Wang, and H. M. Xie, "Generalized spatial-gradient based digital image correlation for displacement and shape measurement with subpixel accuracy," J. Strain Anal. Eng. Des. **44**, 659–669 (2009).
18. B. Pan, H. M. Xie, J. X. Gao, and A. Asundi, "Improved speckle projection profilometry for out-of-plane shape measurement," Appl. Opt. **47**, 5527–5533 (2008).

19. D. Lecompte, A. Smits, S. Bossuyt, H. Sol, J. Vantomme, D. V. Hemelrijck, and A. M. Habraken, "Quality assessment of speckle patterns for digital image correlation," Opt. Lasers Eng. **44**, 1132–1145 (2006).
20. B. Pan, H. M. Xie, Z. Y. Wang, K. M. Qian, and Z. Y. Wang, "Study of subset size selection in digital image correlation for speckle patterns," Opt. Express **16**, 7037–7048 (2008).
21. B. Pan, Z. X. Lu, and H. M. Xie, "Mean intensity gradient: an effective global parameter for quality assessment of the speckle patterns used in digital image correlation," Opt. Lasers Eng. **48**, 469–477 (2010).
22. D. J. Chen, F. P. Chiang, Y. S. Tan, and H. S. Don, "Digital speckle-displacement measurement using a complex spectrum method," Appl. Opt. **32**, 1839–1849 (1993).
23. M. Sjodahl and L. R. Benckert, "Electronic speckle photography: Analysis of an algorithm giving the displacement with subpixel accuracy," Appl. Opt. **32**, 2278–2284 (1993).
24. F. Hild, B. Raka, M. Baudequin, S. Roux, and F. Cantelaube, "Multiscale displacement field measurements of compressed mineral-wool samples by digital image correlation," Appl. Opt. **41**, 6815–6828 (2002).
25. J. Y. Liu and M. Iskander, "Adaptive cross correlation for imaging displacements in soils," J. Comput. Civ. Eng. **18**, 46–57 (2004).
26. J. P. Lewis, "Fast normalized cross correlation," 2003, available at http://www.idiom.com/~zilla/Papers/nvisionInterface/nip.html.
27. J. Y. Huang, T. Zhu, X. Y. Pan, L. Qin, X. L. Peng, C. Y. Xiong, and J. Fang, "A high-efficiency digital image correlation method based on a fast recursive scheme," Meas. Sci. Technol. **21**, 035101 (2010).
28. B. Pan, H. M. Xie, Z. Q. Guo, and T. Hua, "Full-field strain measurement using a two-dimensional Savitzky–Golay digital differentiator in digital image correlation," Opt. Eng. **46**, 033601 (2007).
29. H. Lu and P. D. Cary, "Deformation measurement by digital image correlation: implementation of a second-order displacement gradient," Exp. Mech. **40**, 393–400 (2000).
30. Y. Wang and A. M. Cuitiño, "Full-field measurements of heterogeneous deformation patterns on polymeric foams using digital image correlation," Int. J. Solids Struct. **39**, 3777–3796 (2002).
31. G. Vendroux and W. G. Knauss, "Submicron deformation field measurements. Part 2. Improved digital image correlation," Exp. Mech. **38**, 86–92 (1998).
32. H. Q. Jin and H. A. Bruck, "Theoretical development for pointwise digital image correlation," Opt. Eng. **44**, 067003 (2005).
33. B. Pan, "Reliability-guided digital image correlation for image deformation measurement," Appl. Opt. **48**, 1535–1542 (2009).
34. B. Pan, Z. Y. Wang, and Z. X. Lu, "Genuine full-field deformation measurement of an object with complex shape using reliability-guided digital image correlation," Opt. Express **18**, 1011–1023 (2010).
35. B. Pan, D. F. Wu, and Y. Xia, "High-temperature field measurement by combing transient aerodynamic heating system and reliability-guided digital image correlation," Opt. Lasers Eng. **48**, 841–848 (2010).
36. W. H. Press, *C++ Numerical Algorithms* (Publishing House of Electronics Industry, 2003).
37. H. W. Schreier, J. R. Braasch, and M. A. Sutton, "Systematic errors in digital image correlation caused by intensity interpolation," Opt. Eng. **39**, 2915–2921 (2000).
38. Y. Q. Wang, M. A. Sutton, H. A. Bruch, and H. W. Schreier, "Quantitative error assessment in pattern matching: effects of intensity pattern noise, interpolation, strain and image contrast on motion measurement," Strain **45**, 160–178 (2009).